Dynamics of the Electrochemical Behavior of Diimine Tricarbonyl Rhenium(I) Complexes in Strictly Aprotic Media

Francesco Paolucci,[†] Massimo Marcaccio,[†] Carmen Paradisi,[†] Sergio Roffia,*[,†] Carlo Alberto Bignozzi,[‡] and Christian Amatore[§]

Dipartimento di Chimica, Università di Bologna, Via Selmi 2, 40126 Bologna, Italy and Dipartimento di Chimica, Università di Ferrara, Via Borsari 46, 44100 Ferrara, Italy and Département de Chimie, Ecole Normale Supérieure, URA CNRS 1679, 24 Rue Lohmond, 75231 Paris Cedex 05, France

Received: January 6, 1998

The electrochemical behavior of the family of mononuclear Re(I) complexes, $[Re^{I}(CO)_3LX]^{n+}$, with L = 2,2′-bipyridine (bpy), 1,10-phenanthroline (phen) and X = Cl, CN ($n = 0$); ACN ($n = 1$) and that of the metal−metal-bonded dimeric complexes $[(L)(CO)_3Re-Re(CO)_3(L)]$ (L = bpy, phen) has been studied in various aprotic solvents using cyclic voltammetry (CV), chronoamperometry, and spectroelectrochemistry. The wide cathodic potential window investigated has permitted the observation of the largest number of redox processes so far obtained for these species. A detailed description of the kinetics of both oxidation and reduction processes of such species is given. The electrochemistry of the complexes $[Re(CO)_3(L)CN]$ (L = bpy, phen) is reported here for the first time. The electrochemical behavior of the monomeric species is greatly influenced by the nature of the monodentate ligand X. The concentration dependence of the cyclic voltammetric reductive behavior has evidenced the occurrence of bimolecular homogeneous processes. Such processes include homogeneous electron transfers and the competitive formation of metal−metal or μ-Cl bridged dimeric species. The influence of the solvent and that due to the presence or absence of Cl^- ions in solution is discussed. Digital simulation of the cyclic voltammetric curves is extensively used both for confirming the reaction mechanisms and for the evaluation of the relevant thermodynamic ($E_{1/2}$) and kinetic parameters. Linear correlation between spectroscopic and electrochemical data for the whole family of monomeric and dimeric complexes has been found.

Introduction

The *fac*-$(L)Re^{I}(CO)_3$ chromophore (L = diimine ligand) has received renewed interest in a number of recent studies on the photoinduced intramolecular energy and electron transfer in supramolecular species, in view of the unique combination of features of this chromophore, which include a versatile synthetic chemistry, a high thermal and photochemical stability, luminescent MLCT excited states, and the possibility of systematic tuning of the MLCT energy by suitable choice of the diimine ligand L.[1,2] Most of these works have been devoted to the realization and to the photophysical and photochemical characterization of chromophore−quencher dyads, where *fac*-$(L)Re^{I}(CO)_3$ is the photoactive unit.[1]

In the search of new supramolecular (polynuclear) metal complexes, in which the vectorial energy or electron transfer may be induced by light, this chromophore has recently been chosen for the synthesis of a series of polynuclear Re(I)−Ru(II) complexes of general formula $[Re(CO)_3L(CN)-[Ru(bpy)_2(CN)]_n-Ru(bpy)_2(CN)]^{(n+1)+}$ ($n = 0-2$, L = bpy, phen),[2] whose structural, photophysical, and photochemical characterization has been reported elsewhere.[2] The electrochemical characterization of these species, on the other hand, needs a previous understanding of the electrochemistry of the fundamental components, namely, the *fac*-$(L)Re^{I}(CO)_3-(CN)$ and $-Ru(bpy)_2(CN)_2-$ units. The electrochemical behavior of the latter unit, in the supramolecular frame, has previously been considered,[3] and the effect of the asymmetry of the −CN− bridge on the electrochemical properties has been evidenced.[3] As for the Re(I) unit, the photophysics, photochemistry, and electrochemistry of a great number of diimine tricarbonyl Re(I) complexes have received for the last two decades formidable attention,[4−7] largely prompted by the potential application in solar energy conversion cycles. The interest in these species is derived from the discovery that $[Re(CO)_3bpyCl]$ and analogous complexes may act as both chromophores and homogeneous catalysts in the photocatalytic reduction of CO_2, water, and other small molecules[5] and as electrocatalysts, in the same reactions, either in solution[6] or incorporated in electrode-bound polymer film[7] and, more recently, in Nafion membranes.[7h] Application of a diimine tricarbonyl Re(I) nucleobase complex as luminescent label in DNA sequencing and diagnostics has recently also been proposed.[4x] Despite the great number of investigations devoted to the improvement of the efficiency of the above electrocatalytic cycles, only few studies have dealt with the kinetic details of the complex electrochemical behavior of these species.[6b−d,7e−f] In those works a description of both the oxidative and the reductive behavior of these complexes has been given. As far as the reduction processes are concerned, however, such description is usually restricted to the first two processes due to the limited potential window investigated. Moreover,

* To whom the correspondence should be adressed. E-mail: roffia@ciam.unibo.it.
[†] Università di Bologna.
[‡] Università di Ferrara.
[§] Ecole Normale Supérieure.

S1089-5647(98)00659-2 CCC: $15.00
Published on Web 05/19/1998

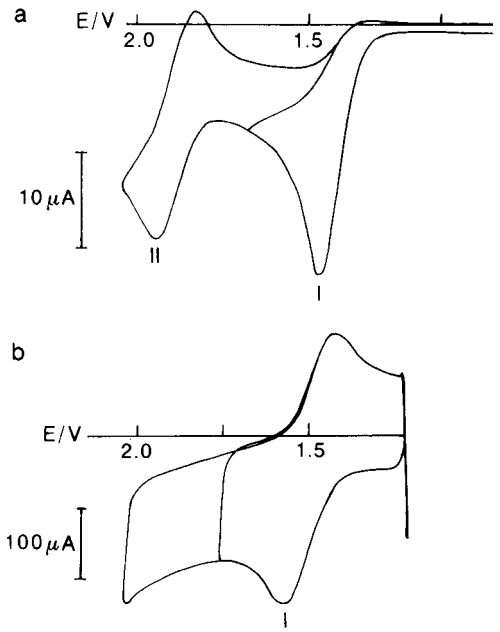

Figure 1. Cyclic voltammetric curves for a 0.5 mM [Re(CO)$_3$bpyCl], 0.05 M TEATFB, ACN solution. $T = 25$ °C. Working electrode: Pt (a) $\upsilon = 0.2$ V/s, (b) $\upsilon = 200$ V/s.

although the influence of the solvent, as well as that of added halide ions and water in the solution, on the photocatalytic efficiency of such species has long been considered,[5g−i,m] detailed electrochemical investigations in solvents other than acetonitrile (ACN) have not so far been carried out.

In the present work, the electrochemical behavior of the family of mononuclear Re(I) complexes, $[Re^{I}(CO)_3LX]^{n+}$, with L = bpy, phen and X = Cl, CN ($n = 0$), ACN ($n = 1$), and that of the metal−metal-bonded dimeric complexes [(L)-(CO)$_3$Re−Re(CO)$_3$(L)] (L = bpy, phen) in aprotic media such as *N*,*N*-dimethylformamide (DMF), ACN, tetrahydrofuran (THF), dichloromethane (CH_2Cl_2), and nitromethane (CH_3NO_2) is discussed.

Results and Discussion

Oxidation Processes. *[Re(CO)$_3$LX]$^{n+}$ (L = bpy, phen; X = Cl, CN (n = 0); X = ACN (n = 1).* The CV curve shown in Figure 1a, relative to a 0.5 mM [Re(CO)$_3$bpyCl] ACN solution, at 25 °C and a scan rate (υ) of 0.2 V/s, shows two one-electron peaks, labeled I and II, the first one, with $E_p^{I} = 1.39$ V, irreversible and the second one reversible, with $E_{1/2}^{II} = 1.79$ V. By increasing the scan rate, the first peak gradually gains reversible features and, at the same time, the height of the second peak gradually decreases, eventually disappearing, at $\upsilon \geq 200$ V/s (Figure 1b), when the first peak attains full reversibility ($E_{1/2}^{I} = 1.40$ V). The same voltammetric behavior is shown by the complex in which a phen ligand was substituted for a bpy. In this case, $E_{1/2}^{I} = 1.41$ and $E_{1/2}^{II} = 1.82$ V.

From the observed CV behavior as a function of scan rate the first oxidation process is described as chemically irreversible (EC mechanism) with a first-order following reaction by which the electroactive species responsible for peak II is generated. From the digital simulation of the CV curves based on this mechanism the value for the first-order rate constant *k* for both [Re(CO)$_3$bpyCl] and [Re(CO)$_3$phenCl] was 30 ± 6 s^{-1}. The coincidence of the values of *k* for the two complexes indicates no significant effect due to the nature of the bidentate diimine ligand. Conversely, a strong effect was observed replacing the chloride ligand with cyanide. The CV curves of [Re(CO)$_3$bpyCN] and [Re(CO)$_3$phenCN] closely resembled those of the respective chloro complexes; however, (i) process I occurs at more positive potentials for the cyanide complexes ($E_{1/2}$ values are 1.56 and 1.60 V for [Re(CO)$_3$bpyCN] and [Re(CO)$_3$phenCN], respectively), (ii) the chemical step following the oxidation process is faster in the cyanide complexes (the first-order rate constant value increased to $k = 70 \pm 10$ s^{-1} for both [Re(CO)$_3$bpyCN] and [Re(CO)$_3$phenCN]). By contrast $E_{1/2}^{II}$ values for both cyanide complexes coincide with those for the respective chloride complexes (1.79 V for [Re(CO)$_3$bpyCN] and 1.82 V for [Re(CO)$_3$phenCN]). The product generated following oxidation I is therefore identified with the oxidized complex having lost either the cyanide or the chloride ligand. Notice that both chloride and cyanide ions are (irreversibly) oxidized at $E \geq 1.0$ V under the present experimental conditions and that therefore they must leave the oxidized complexes as radicals rather than as anions. In the latter case, in fact, peak I would comprise two electrons/molecule, being both the metal and the ligand oxidized according to a E_1CE_2 mechanism ($E^\circ_{\ 2} < E^\circ_{\ 1}$), in contrast with the experimental evidence. CV experiments carried out in the presence of excess diimine ligand (phen or bpy) or in saturated CO solution showed no significant change of the curve morphology excluding the concomitant (reversible) loss of such ligands during the process. Rapid coordination of a ACN molecule is instead assumed to occur generating the solvato complex $[Re^{I}(CO)_3L(ACN)]^+$, which is in turn responsible for peak II. This is in line with the recently reported in situ infrared spectroelectrochemical investigation relative to [Re(CO)$_3$dmbpyCl] (dmbpy = 4,4′-dimethylbpy)[6d] and was confirmed in the present study by comparison with authentic samples of $[Re(CO)_3phen(ACN)]^+$ and $[Re(CO)_3bpy(ACN)]^+$. The CV curves relative to these species, under the conditions of Figure 1a, show a single reversible oxidation peak, attributed to the Re(I) → Re(II) oxidation[4d,6d,7e,f] and coinciding with peak II in the CV curves of the corresponding phen and bpy chloride and cyanide complexes.

Finally, the nature of the solvent was found to be noninfluential on the kinetics coupled to peak I for both chloride and cyanide complexes. Owing to the wide span of donor properties investigated (donor numbers (DN) are 0, 2.7, and 14.1 kcal/mol for CH_2Cl_2, CH_3NO_2, and ACN), this either excludes that loss of Cl or CN from $[Re(CO)_3LX]^+$ may be concerted with coordination of ACN or that solvent molecule uptake is the rate-determining step in a stepwise mechanism.

Reduction Processes. The study of the cathodic processes was carried out, unless otherwise stated, at −54 °C. The use of low temperatures and strictly aprotic conditions allowed in fact obtaining wide cathodic ranges and the observation of the largest number of reduction processes and a detailed description of the kinetics associated with the reduction processes of the title complexes. The behavior at room temperature was found not to differ significantly from that at low temperature except for the higher rate at which the chemical reactions associated with charge transfers occur.

[Re(CO)$_3$LCN] (L = bpy, phen). The CV curve for a 0.5 mM [Re(CO)$_3$bpyCN], at −54 °C and $\upsilon = 0.2$ V/s is shown in Figure 2a. Two one-electron reversible diffusion controlled redox processes are observed, labeled I and II, with $E_{1/2}^{I} = -1.30$ V and $E_{1/2}^{II} = -1.95$ V. The potential separation between the two redox processes (650 mV) is a typical value for successive reductions centered in diimine ligands in both the free and coordinated state.[3,8] The two reductions give therefore $[Re(CO)_3(bpy)CN]^-$ and $[Re(CO)_3(bpy)CN]^{2-}$, re-

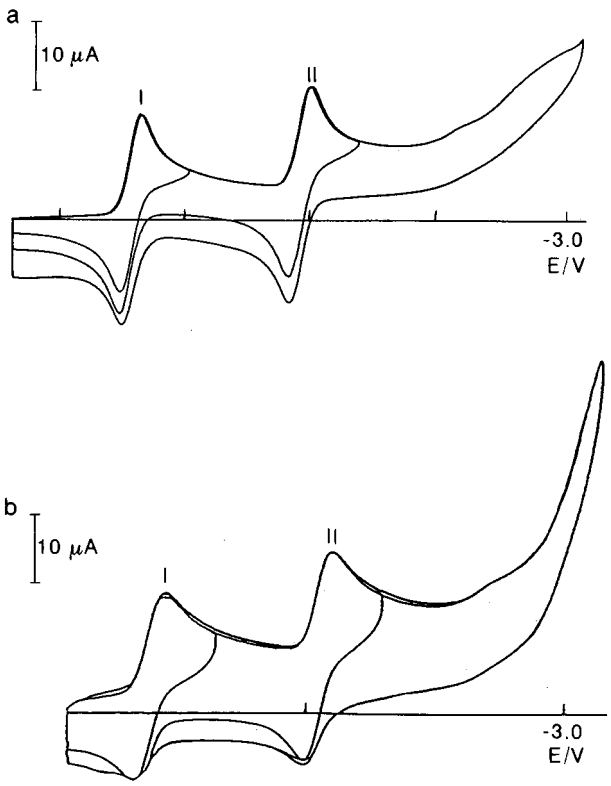

Figure 2. Cyclic voltammetric curves for 0.5 mM (a) [Re(CO)$_3$bpyCN], (b) [Re(CO)$_3$phenCN], 0.05 M TEATFB, DMF solutions. $T = -54$ °C, $v = 0.2$ V/s. Working electrode: Pt.

spectively, in which the metal retains its +1 oxidation state. Confirmation of this attribution is derived by a comparison with the homologous complex [Re(CO)$_3$phenCN]. The same CV pattern was in fact observed with $E_{1/2}^{I} = -1.42$ V and $E_{1/2}^{II} = -2.05$ V, respectively (Figure 2b). The negative shift of the first reduction of [Re(CO)$_3$phenCN] and the slightly larger separation between the two reductions with respect to the bpy homologues match the differences observed between the non-coordinated ligands. Summarizing, the reductive behavior of tricarbonyl cyanide Re(I) complexes resembles that typical of polyimine complexes of other transition metals such as Ru(II) and Os(II).[9] This result is quite interesting in view of the notable differences observed in the case of the complexes where a low-field ligand replaces CN, described in the following section.

[Re(CO)$_3$bpyX]$^{n+}$ (X = Cl, n = 0; X = ACN, n = 1); [Re(CO)$_3$bpy]$_2$. The CV curve for a 0.5 mM solution of [Re(CO)$_3$bpyCl] in DMF at $v = 0.2$ V/s and $T = -54$ °C is reported in Figure 3a. Four reduction peaks are observed, labeled by increasing Roman numbers, each corresponding to a one-electron charge transfer. Peaks I, III, and IV are electrochemically reversible (with $E_{1/2} = -1.38$, -2.49, and -2.73 V) as proved by the presence of the corresponding anodic peaks (B, D, and E, for peak B; see also Figure 3b) within the expected potential interval. While for peaks I and III the values of i_{pa}/i_{pc}, where i_{pa} and i_{pc} represent the anodic and cathodic peak heights, are close to unity, indicating their chemical reversibility (Figure 3b,c), for peak IV this is true only at $v \geq 2$ V/s. At the same time, two anodic peaks indicated by asterisks in Figures 3 are observed at lower scan rates than 2 V/s when the inversion potential approaches and passes peak IV (Figure 3c). This indicates the occurrence of a slow followup reaction coupled to peak IV (EC mechanism). Peak II corresponds to an electrochemically reversible but chemically totally irreversible process. A fast irreversible followup reaction affects reduction II, whose rate constant was estimated by digital simulation of the CV curve (vide infra) to be greater than 10^5 s^{-1}. Anodic *wave* (rather than *peak*) C is not the anodic counterpart of peak II, as it will be shown below. In the reverse scan, at more positive potentials than peak B, anodic peak A is observed. The heights of wave C and of peak A gradually increase as the inversion potential approaches peak II, Figure 3b, at the expense of that of peak B, the anodic counterpart of peak I. This behavior is consistent with the fact that wave C and peak A are due to the same species generated from the starting complex after peak II. The two small peaks, indicated by An, are due to residual anthracene present in the purified solvent (see Experimental Section).

As shown in the multiscan CV curve in Figure 4a, obtained under the conditions of Figures 3a−c, without the renewal of the diffusion layer, both wave C and peak A have a cathodic counterpart (denoted by V and VI, respectively), unobserved during the first scan.

Peaks VI and A comprise a Nernstian redox couple with $E_{1/2} = -1.20$ V. The same is not true for peak V and wave C, and the mechanism associated with this redox process will be discussed in the following. The presence of several isopotential points (IPPs) in the CV curves indicates that the conversion of the pristine complex (peaks I and II) to the new electroactive species (peaks VI and V) occurs in the voltammetric time scale without any loss of electroactive material, the sum of the reactant and product concentrations remaining constant. The presence of IPPs in the CV curve has found analogous interpretation in many cases.[10] The conservation of electroactive mass on the CV time scale was independently checked by double-step chronoamperometric experiments. The potential was stepped from an initial value (−1.00 V), at which no reduction process occurred, to −2.00 V, corresponding to the diffusion-controlled two-electron reduction of [Re(CO)$_3$bpyCl]. After a time τ, the current $i_f(\tau)$ was measured and the potential was stepped back to the initial value where the electroactive products of the two-electron reduction are reoxidized. Then, after the identical time τ from the second step, the current $i_r(2\tau)$ was measured. The expected value for the ratio $i_r(2\tau)/i_f(\tau)$, in the case of a reversible process, is $0.293/n$ (n is the number of electrons exchanged in the process),[11] and the same value is expected, also in the presence of kinetic complications, when the total concentration of the electroactive species is not altered by the interposed chemical reactions. In the present case, the value of $i_r(2\tau)/i_f(\tau)$, invariant with τ for step durations comparable to that of the CV experiments, was 0.146 ± 0.05, in excellent agreement with the expected value for $n = 2$. No loss of electroactive mass is therefore occurring during the (micro)electrolysis.

Wave C has a shape that is typical of redox processes whose rate is controlled by a preceding chemical reaction (CE mechanism).[12,13] Since the reaction coupled to peak II is very fast, it cannot be the rate-determining step, and a slow reaction, successive to that fast reaction and prior the anodic electron transfer, has to be considered. This was demonstrated by performing the numerical simulation of the CV curve, calculated under the conditions of Figure 4a and based on the opposite hypothesis that no such slow reaction occurs. The fit of the resulting curve, shown in Figure 4b, with the experimental one was rather poor especially as regards wave C. In the simulation, Nernstian electron-transfer kinetics were considered and the rate constant for the above chemical step was set to 10^5 s^{-1}. The $E_{1/2}$ values used were obtained from the CV curves as far as peaks I/B and VI/A are concerned, and for reduction II it was adjusted so as to obtain, in the simulated curve, the experimental E_p at 0.2 V/s.

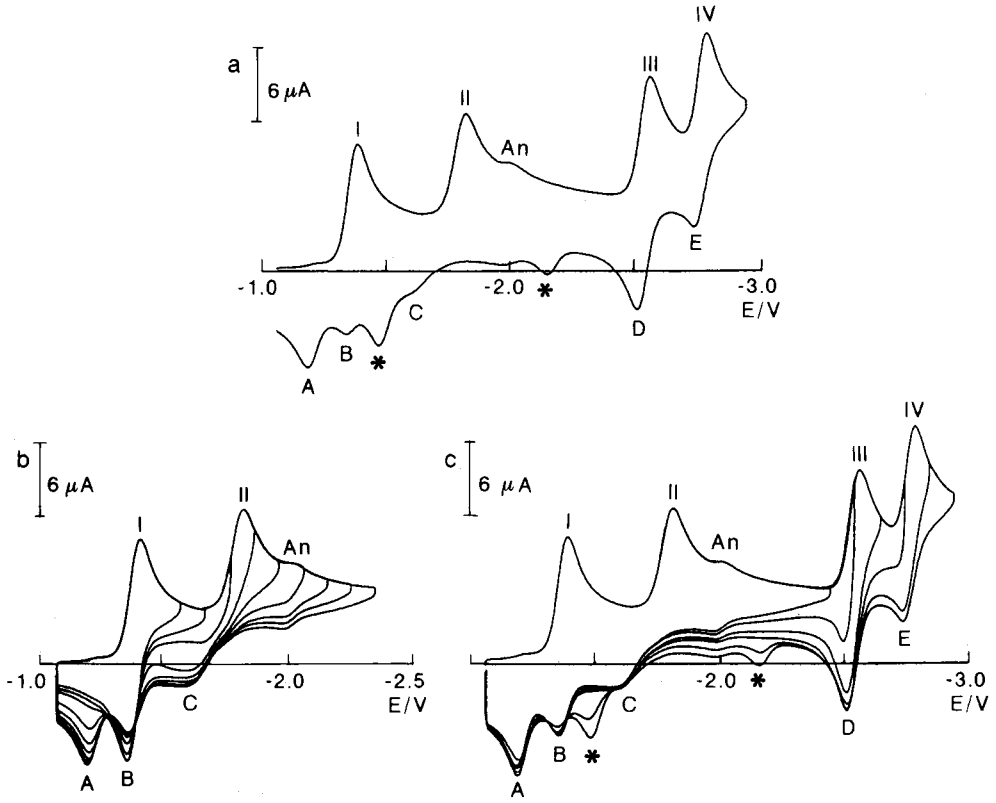

Figure 3. Cyclic voltammetric curves for a 0.5 mM $[Re(CO)_3bpyCl]$, 0.05 M TEATFB, DMF solution. $T = -54$ °C, $v = 0.2$ V/s. Working electrode: Pt.

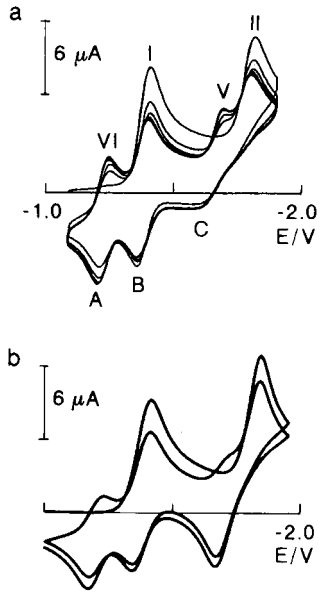

Figure 4. (a) Multiscan cyclic voltammetry for a 0.5 mM $[Re(CO)_3bpyCl]$, 0.05 M TEATFB, DMF solution. $T = -54$ °C. $v = 0.2$ V/s. Working electrode: Pt. (b) Simulated cyclic voltammetric curve according to the mechanism outlined in the text, under the conditions of Figure 4a. Only the first two cycles are shown.

Another effect that had to be accounted for was the dramatic dependence of the CV curve pattern on concentration. The concentration effects are illustrated in Figure 5, obtained under the conditions of Figures 3a−c and 4a but with an increased concentration of $[Re(CO)_3bpyCl]$ from 0.5 to 2.0 mM.

The most significant differences between the high-concentration and the corresponding low-concentration curves are the following: (i) wave C is replaced by the broad anodic peak C with $E_p = -1.65$ V (at 0.2 V/s); (ii) the height of peaks A and VI increases at the expense of that of peaks B and $i_{pI,2nd}$, respectively, where $i_{pI,2nd}$ is the height of peak I in the second scan CV curve: i_{pA}/i_{pB} changes (at 0.2 V/s) from 0.8 to 1.5 and $i_{pVI}/i_{pI,2nd}$ from 0.5 to 1, passing from low to high concentrations. Finally, (iii) the height of peak I decreases in the multicycle CV curves sooner at high concentration than at low concentration. The ratio $i_{pI,2nd}/i_{pI,1st}$ is in fact 0.7 at low concentration and 0.5 at high concentration (at 0.2 V/s). By contrast, the remaining part of the CV curve, in particular that relative to the processes occurring beyond peak II, is not affected by the concentration change. Quite interestingly, at high concentration, features similar to those observed at low concentration were obtained by increasing the scan rate ($v \geq 1$ V/s). Conservation of electroactive mass in the CV time scale was also in this case proved by double-step chronoamperometry.

The observed dependence of the CV curve on the complex concentration urged the inclusion of homogeneous reactions with order greater than one with respect to the complex in the reaction scheme. These reactions should provide a homogeneous pathway for increasing the concentrations, in the diffusion layer, of the species responsible for wave C and peaks A, V, and VI at the expense of the pristine complex responsible for peaks I and B.

The minimal mechanism that accounts for the observed CV behavior is illustrated in Scheme 1. Using the symbols of Scheme 1, such homogeneous reactions should increase the concentration of **5** and **6** at the expense of that of **1** and **2**. This may in principle result from the occurrence of solution (homogeneous) electron-transfer (SET) reactions involving the above species. The important role played by SET reactions in electrode mechanisms such as that in Scheme 1 has long been assessed.[14] Among the various conceivable SET reactions compatible with Scheme 1, those expected to have the desired

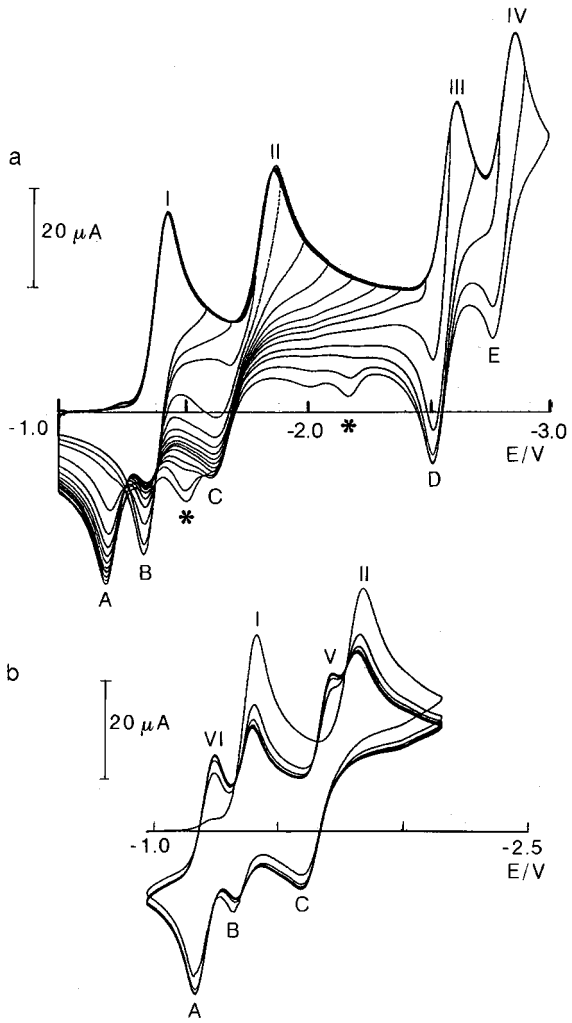

Figure 5. (a) Cyclic voltammetric curves and (b) multiscan cyclic voltammetric curve for a 2.0 mM [Re(CO)$_3$bpyCl], 0.05 M TEATFB, DMF solution. $T = -54$ °C, $v = 0.2$ V/s. Working electrode: Pt.

SCHEME 1

1 ⇔ **2** ⇔ **3**
↓ **fast**
4 ⇔ **8** ⇔ **9**
$\mathbf{k_5}\downarrow\uparrow\mathbf{k_{-5}}$
7 ⇔ **6** ⇔ **5**

effect on the intermediate concentrations are reactions 1−4.

$$\mathbf{1} + \mathbf{5} \leftrightarrow \mathbf{2} + \mathbf{6} \quad (1)$$

$$\mathbf{2} + \mathbf{5} \leftrightarrow \mathbf{3} + \mathbf{6} \quad (2)$$

$$\mathbf{1} + \mathbf{4} \leftrightarrow \mathbf{2} + \mathbf{6} \quad (3)$$

$$\mathbf{2} + \mathbf{4} \leftrightarrow \mathbf{3} + \mathbf{6} \quad (4)$$

It should be noted that in SET reactions 3 and 4 the assumption is made that homogeneous oxidation of **4** leads to the same product **6** obtained when **5** is involved. The nature of species **4** and **5** will be further discussed in the following. Inclusion of reactions 1 and 2 in the mechanism of Scheme 1 did not have the desired effect on the simulated curve. In particular, its pattern was insensitive to the concentration. On the other hand, by introducing reactions 3 and 4, a rather satisfactory agreement between calculated and experimental curves was obtained. In particular, the simulated CV pattern changed significantly, and in the desired direction, with the complex concentration. Peak height ratios i_{pA}/i_{pB} relative to the simulated CV curves close to the experimental values were obtained, by a suitable choice of the simulation parameters, at both low and high concentration. However, with any choice of the rate constants relative to reactions 3 and 4, the simulation failed to reproduce the concentration effect on shape and corresponding charge of peak C, which was always lower than in the experiment. The correct concentration effect was only reproduced in the calculated curves assuming that the chemical step leading from species **4** to **5** was in fact itself sensitive to concentration, i.e. a bimolecular reaction involving two molecules of **4**:

$$\mathbf{4} + \mathbf{4} \leftrightarrow \mathbf{5} \quad (5)$$

According to CV and chronoamperometric results, which show no loss of electroactive species during the two-electron reduction of [Re(CO)$_3$bpyCl], and since reaction 5 is formally a dimerization reaction that halves the complex concentration, the successive oxidation of **5** does necessarily occur either (i) as a two-electron process followed by dissociation into two molecules of **6** (eqs 6−6′) or (ii) as a one-electron process followed by dissociation into one molecule of **5** and one of **4** (eqs 7−7′).

$$\mathbf{5} \leftrightarrow \mathbf{5}^{2+} + 2e \quad (6)$$

$$\mathbf{5}^{2+} \rightarrow \mathbf{6} + \mathbf{6} \quad (6')$$

$$\mathbf{5} \leftrightarrow \mathbf{5}^{+} + e \quad (7)$$

$$\mathbf{5}^{+} \rightarrow \mathbf{6} + \mathbf{4} \quad (7')$$

Inclusion of either reactions 6/6′ or 7/7′ into the reaction mechanism of Scheme 1, together with the SET reactions 3−4, allowed obtaining a very good agreement between calculated and experimental curves. The use of reactions 7/7′ gave however the best concentration dependence of shape and charge of wave/peak C in the simulations. The simulated curves, under the conditions of Figures 4a and 5b are shown in Figures 6a and 6b, respectively. The kinetic parameters used in the simulation were $k_3 = 4 \times 10^3$ M^{-1} s^{-1}, $k_{-3} = 10^{-3}$ M^{-1} s^{-1}; $k_4 = 4 \times 10^2$ M^{-1} s^{-1}, $k_{-4} = 2 \times 10^5$ M^{-1} s^{-1}; $k_5 = 10^3$ M^{-1} s^{-1}, $k_{-5} = 4 \times 10^4$ s^{-1}; $k_{7'} \geq 10^5$ s^{-1}. It is important to stress the fact that curves a and b in Figure 6 were obtained *using the same set of simulation parameters* and changing only the concentration of the starting species by the same amount as in the respective experiments.

Let's now consider the remaining part of the CV curve shown in Figures 3 and 5. Peaks III and IV correspond, in the whole range of scan rates investigated (0.1−1000 V/s), to one-electron, diffusion-controlled reductions. Their height was unaffected by any change of complex concentration and always remained equal to that of peak I. This result excludes that peaks III and IV are successive reductions of **5** (Scheme 1), since a marked concentration dependence of these processes would be expected in that case. The redox processes are therefore attributed to the two successive reductions of **4** (Scheme 1) according to the following equations:

$$\mathbf{4} + e \leftrightarrow \mathbf{8} \quad (8)$$

$$\mathbf{8} + e \leftrightarrow \mathbf{9} \quad (9)$$

We shall address now the problem of identifying species **1**−**9** in Scheme 1. Species **1**, **2**, and **3** represent the parent

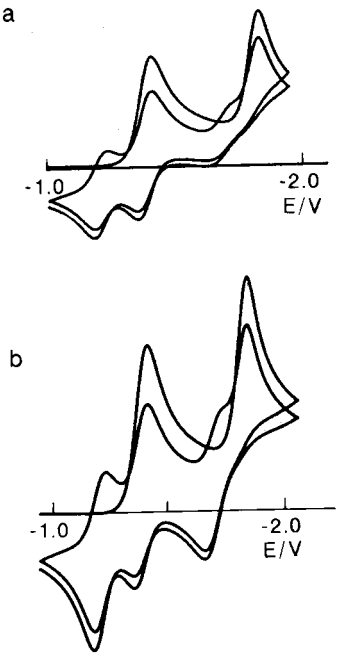

Figure 6. Simulated cyclic voltammetric curves according to the mechanism in Scheme 1 (see text) under the conditions of Figures 4a and 5b. (a) [Re] = 0.5 mM; (b) [Re] = 2.0 mM, υ = 0.2 V/s.

complex in three different oxidation states: $[Re(CO)_3bpyCl]$, $[Re(CO)_3bpyCl]^{\bullet-}$, and $[Re(CO)_3bpyCl]^{2-}$. As to the location of the transferred electrons in the molecule, it has been long stated that the first reversible reduction of halotricarbonyl Re(I) complexes containing diimine ligands such as bpy, phen, and 2,2′-biquinoline is invariably located onto the diimine ligand.[6,4l] A confirmation of such location was obtained, in the present study, from the correlation of electrochemical and spectroscopic data shown in the following section. The second electron, by contrast, would enter the metal-centered dσ* (Re−halide antibonding) orbital, bringing about the rapid cleavage of the Re−halide bond.[6] As shown above, such behavior was not observed in $[Re(CO)_3bpyCN]$ and $[Re(CO)_3phenCN]$. In that case, the high-field cyanide ligand shifts the metal-centered dσ* orbital to higher energies and the second electron couples with the first one in the same π* diimine-centered orbital rather than entering the dσ* one. In the case of $[Re(CO)_3bpyCl]$, by contrast, free Cl^- was detected after its irreversible two-electron reduction in ACN. Although direct detection of free Cl^- in the solution was not achievable in DMF due to its narrower anodic limit, identification of species **4** as $[Re(CO)_3(bpy)]^-$ was obtained by a comparison with the CV behavior of $[bpy(CO)_3Re-Re(CO)_3bpy]$ and $[Re(CO)_3bpy(ACN)]^+$ under the same conditions (vide infra). $[Re(CO)_3(bpy)]^-$ might in principle undergo a fast solvation leading to the solvato complex $[Re(CO)_3(bpy)(DMF)]^-$. The formation of the solvato complex was proved not to occur in ACN in the case of $[Re(CO)_3dmbpyCl]$ (dmbpy = 4,4′-dimethylbpy).[6d] However, owing to the different donating properties of DMF with respect to ACN, solvent coordination might occur in the present case. In this case, peaks III and IV would correspond to the two successive reversible reductions of $[Re(CO)_3(bpy)(DMF)]^-$. A significant shift of the corresponding $E_{1/2}$ values should therefore be expected in DMF with respect to other solvents. The same four reduction peaks pattern, with similar characteristics as in DMF, was observed in ACN and THF. The first peak was not much affected by the change of solvent ($E_{1/2}$ = −1.38, −1.36, and −1.35 V in DMF, ACN, and THF, respectively). The potential of peak II changed from −1.78 and −1.80 V in DMF and ACN, respectively, to −1.90 V in THF (at 0.2 V/s). The $E_{1/2}$ values relative to peaks III and IV, −2.49 and −2.73 V in DMF, were −2.46 and −2.73 V in ACN and −2.50 and −2.79 V in THF. These values were therefore only slightly influenced by the change of solvent, and the observed shift seems to parallel the variation in the dielectric constant (DMF 36.1, ACN 38.0, and THF 7.6)[15] rather than the change in donor properties (DN = 26.6, 14.1, and 20.0 kcal/mol, for DMF, ACN, and THF, respectively). This suggests that the energetics of the reduction processes involving $[Re(CO)_3(bpy)]^-$ is mainly dominated by ion−solvent interactions and that the formation of a solvato complex does not occur. Species **8** and **9** in Scheme 1 are therefore identified as $[Re(CO)_3bpy]^{2-}$ and $[Re(CO)_3bpy]^{3-}$, respectively. According to the above location of the first and second reduction of $[Re(CO)_3bpyCl]$, processes 7 and 8 should correspond to one metal-centered followed by one ligand-centered reduction, leading eventually to the species $[Re^{-I}(CO)_3(bpy^{2-})]^{3-}$ (18-electron species). If, on the other hand, an intramolecular electron transfer occurred in the doubly reduced pentacoordinated species **4** ($[Re^0(CO)_3(bpy^-)]^{\bullet-}$, 17-electron) leading to the isoelectronic $[Re^{-I}(CO)_3(bpy)]^-$ (18-electron), the two successive reductions would both locate into bpy. This would however contrast with the small separation between the two redox processes, 240, 270, and 290 mV in DMF, ACN, and THF, respectively, which is significantly smaller than the expected coupling separation between two successive reductions of a diimine ligand in transition metal complexes, ca. 600 mV (650 mV in $[Re(CO)_3bpyCN]$, vide supra).[3,8]

To confirm the above attributions and, at the same time, to identify species **5**, **6**, and **7** in Scheme 1, the CV behavior of $[bpy(CO)_3Re-Re(CO)_3bpy]$ and $[Re(CO)_3bpy(ACN)]^+$, under the conditions used for $[Re(CO)_3bpyCl]$, was investigated. The CV curves relative to a 1 mM solution of $[bpy(CO)_3Re-Re(CO)_3bpy]$, in DMF at −54 °C and υ = 0.2 V/s, are shown in Figure 7a,b. The CV curve in Figure 7a strikingly resembles that relative to the 2 mM solution of $[Re(CO)_3bpyCl]$ (Figure 5a). In particular, four reduction peaks are observed, peaks I, III, and IV reversible, with $E_{1/2}$ = −1.56, −2.49, and −2.73 V, respectively, and the second, peak II, irreversible, with E_p = −1.86 V (0.2 V/s). The kinetic analysis of peak II showed, analogously to what is observed for $[Re(CO)_3bpyCl]$, the chemical nature of its irreversibility (EC mechanism). The first-order rate constant relative to the chemical step was estimated to be again greater than 10^5 s^{-1}. Moreover, although the $E_{1/2}$ relative to peak I and the E_p of peak II for $[bpy(CO)_3Re-Re(CO)_3bpy]$ and $[Re(CO)_3bpyCl]$ are significantly different, the $E_{1/2}$ values relative to peaks III and IV coincide for the two species. Moreover, for $[bpy(CO)_3Re-Re(CO)_3bpy]$, the heights of peaks III and IV are twice that of peak I.

The above characteristics suggest that the second, chemically irreversible, reduction of $[bpy(CO)_3Re-Re(CO)_3bpy]$ brings about the homolytic cleavage of the Re−Re bond, giving the species $[Re(CO)_3bpy]^-$ also generated in the case of $[Re(CO)_3bpyCl]$. The cleavage produces two identical fragments from each doubly reduced dimer: the observed double heights of peaks III and IV are therefore explained. The comparison between the CV curves of the dimer and $[Re(CO)_3bpyCl]$ was particularly interesting as far as the dynamics of reoxidation of the $[Re(CO)_3bpy]^-$ fragment is concerned. For $[Re(CO)_3bpy]^-$ generated from the dimer, due the initial concentration of the latter (1 mM), a CV behavior analogous to that observed in the case of $[Re(CO)_3bpyCl]$ at high concentration (2 mM) is expected relative to the oxidation processes corresponding to

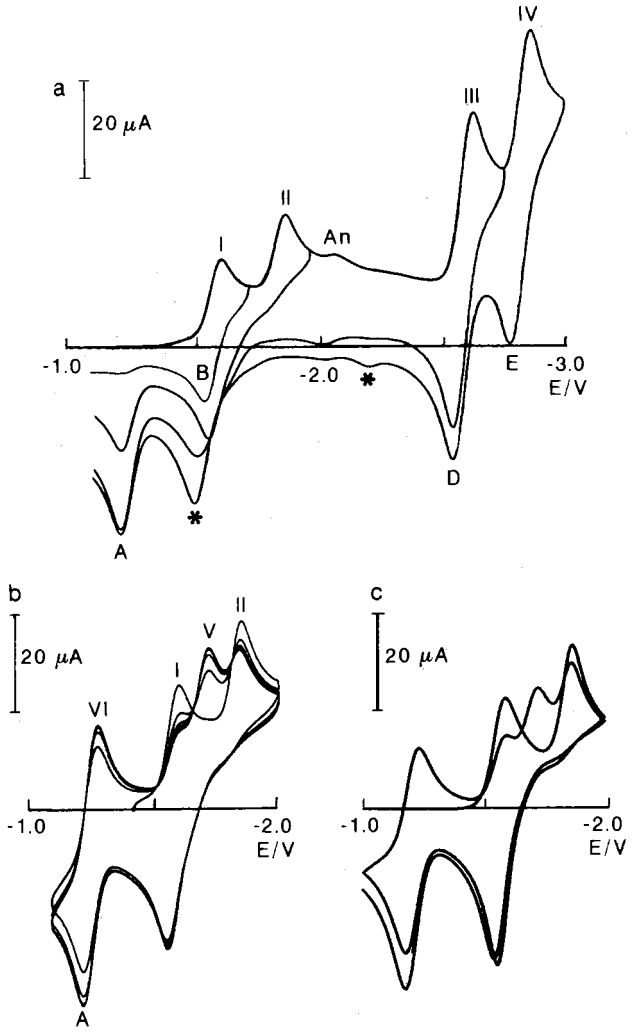

Figure 7. Single cycle (a) and multiscan (b) cyclic voltammetric curves for a 1.0 mM $[Re(CO)_3bpy]_2$, 0.05 M TEATFB, DMF solution. $T = -54$ °C, $\upsilon = 0.2$ V/s. Working electrode: Pt. (c) Simulated cyclic voltammetric curve according to the mechanism in Scheme 1 (see text), under the conditions of Figure 7b. Only the first two cycles are shown.

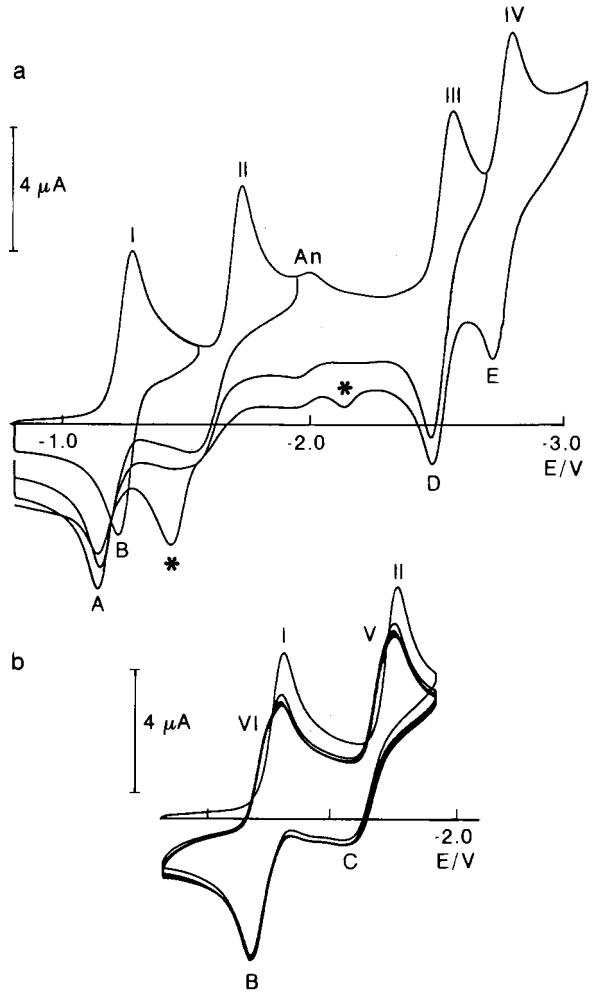

Figure 8. Single-cycle (a) and multiscan (b) cyclic voltammetric curves for a 2.0 mM $[Re(CO)_3bpyACN]TFB$, 0.05 M TEATFB, DMF solution. $T = -54$ °C, $\upsilon = 0.2$ V/s. Working electrode: Pt.

peaks VI/A and V/C. In Figure 7, peak C is partly overlapping with peak B (the anodic counterpart of peak I), making a comparison with $[Re(CO)_3bpyCl]$ difficult: a single anodic peak is in fact observed, between −1.45 and −1.55 V depending on the inversion potential and whose height corresponds to more than 1 electron/molecule, compatible with the dissociation of $[bpy(CO)_3Re-Re(CO)_3bpy]^{2-}$ into two $[Re(CO)_3bpy]^-$ fragments. The numerical simulation of the CV curve relative to the dimer, based on the mechanism in Scheme 1, with the relevant $E_{1/2}$ values and considering the homolytic dissociation of $[bpy(CO)_3Re-Re(CO)_3bpy]^{2-}$ was therefore carried out. The same set of kinetic parameters used for the simulated curve in Figure 6b (high concentration) was used. The agreement with the experimental curve at the level of peak B and C was however rather poor. In particular, instead of a single peak, a well-defined doublet of anodic peaks corresponding to the oxidation of **5** (peak C) and **2** (peak B), respectively, was obtained. A better agreement between the simulated and the experimental curve, Figure 7c, was instead obtained, within the same mechanism of Scheme 1, with a much lower value for k_5 (10 M^{-1} s^{-1}). This was totally unexpected since the species involved in reaction 5 is the same for $[Re(CO)_3bpyCl]$ and $[bpy(CO)_3Re-Re(CO)_3bpy]$, and also the concentrations coincide in the two cases. Quite interestingly, analogous results were obtained with the complex $[Re(CO)_3bpyACN]^+$. Figure 8 shows the CV curves obtained for a 2 mM solution of $[Re(CO)_3bpyACN]^+$ in DMF and under the conditions of Figure 5.

The CV curve pattern is very similar to that of $[Re(CO)_3bpyCl]$. In particular, peaks I, III, and IV correspond to one-electron diffusion-controlled reductions with $E_{1/2} = -1.26$, −2.50, and −2.73 V, while peak II is irreversible. The coincidence of the $E_{1/2}$ for peak III and IV with the corresponding peaks in $[Re(CO)_3bpyCl]$ and $[bpy(CO)_3Re-Re(CO)_3bpy]$ suggests that, also for $[Re(CO)_3bpyACN]^+$, the species $[Re(CO)_3bpy]^-$ is involved. Such species, in the present case, would be generated upon the irreversible loss of ACN from $[Re(CO)_3bpyACN]^-$. As to the reoxidation processes involving this species, the same pattern as for $[Re(CO)_3bpyCl]$ and $[bpy(CO)_3Re-Re(CO)_3bpy]$ is observed. The relative oxidation peaks are however partly masked by those involving the pristine species for the near coincidence of the relative $E_{1/2}$ values. Moreover, a low wave C resembling that of the low concentration CV curve of $[Re(CO)_3bpyCl]$ is observed. The CV behavior of $[Re(CO)_3bpyACN]^+$ may be described according to the same mechanism in Scheme 1 as confirmed by the digital simulation of the CV curve. The value for k_5 used in the simulation was however close to that used in the case of the dimer indicating that also in this case the dynamics of oxidation

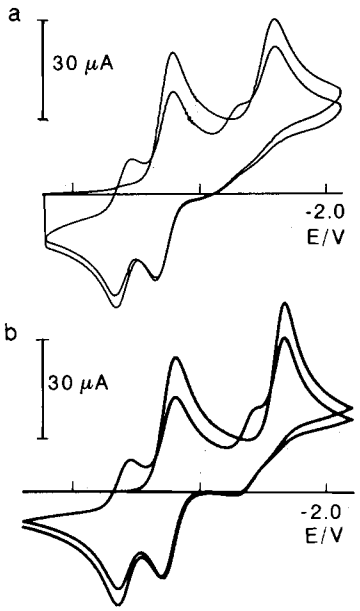

Figure 9. (a) Two-scan cyclic voltammetric curve for a 2.0 mM [Re(CO)$_3$bpyCl], 0.05 M NaTFB, DMF solution. $T = -54$ °C, $\upsilon = 0.2$ V/s. Working electrode: Pt. (b) Simulated CV curve according to the mechanism in Scheme 1 (see text).

of [Re(CO)$_3$bpy]$^-$ differs significantly from that observed for [Re(CO)$_3$bpyCl].

On the basis of the above observations, the hypothesis is advanced that Cl$^-$ ions, released in the diffusion layer in the case of [Re(CO)$_3$bpyCl] and absent for the other two complexes, are directly involved in the heterogeneous oxidation of [Re(CO)$_3$bpy]$^-$. This hypothesis was tested by addition of Na$^+$ ions to the [Re(CO)$_3$bpyCl] DMF solution. This was meant to efficiently remove the released Cl$^-$ ions via the formation of unsoluble NaCl. The experiment, carried out under the conditions of Figure 5 (high concentration), but using NaTFB instead of TEATFB as supporting electrolyte (Figure 9a), unequivocally confirmed the fundamental role played by Cl$^-$ in the oxidative behavior of [Re(CO)$_3$bpy]$^-$.

In the presence of Na$^+$ ions, instead of the broad peak C observed in Figure 5, a low wave resembling that in the low concentration CV curve (Figure 3) was obtained. At the same time, addition of Na$^+$ also affected peaks VI/A and V, whose heights decreased with respect to those in Figure 5. The digital simulated curve, relative to the CV curve in Figure 9a, is shown in Figure 9b and was obtained with the same set of simulation parameters used for the simulated curve in Figure 6b except for k_5, which was set to the value used for the simulation of the CV curves of the dimer and of the acetonitrile complex. Notice that in the case of [bpy(CO)$_3$Re−Re(CO)$_3$bpy] and [Re(CO)$_3$bpyACN]$^+$ no significant change in the CV curve was observed upon addition of Na$^+$.

A possible explanation for the observed unique role played by Cl$^-$ in the heterogeneous oxidation of [Re(CO)$_3$bpy]$^-$ is the formation of a μ-Cl-bridged intermediate. In a study relative to the atom-transfer reaction between the radical [Re(CO)$_4$L]$^\bullet$ (L = P(CH$_3$)$_3$, P(O-i-C$_3$H$_7$)$_3$), generated by N_2 laser flash photolysis, and a series of organic halides RX (X = Cl, Br, I),[16] it has been shown that the rate-limiting step is represented by an inner-sphere electron transfer involving the μ-X-bridged species {R···X···[Re(CO)$_4$L]}. In analogy to this mechanism, the heterogeneous oxidation of [Re(CO)$_3$bpy]$^-$ is thought to occur through the formation of the analogous μ-Cl intermediate {(bpy)Re···Cl···Re(bpy)}$^{3-}$ (where the carbonyls are omitted for clarity). Equations 5 and 7/7′ should be written accordingly as follows:

$$2[(bpy)Re]^{\bullet -} + Cl^- \leftrightarrow \{(bpy)Re\cdots Cl\cdots Re(bpy)\}^{3-} \quad (10)$$

$$\{(bpy)Re\cdots Cl\cdots Re(bpy)\}^{3-} \Leftrightarrow \{(bpy)Re\cdots Cl\cdots Re(bpy)\}^{2-} + e \quad (11)$$

$$\{(bpy)Re\cdots Cl\cdots Re(bpy)\}^{2-} \Leftrightarrow [Re(bpy)]^\bullet + [Re(bpy)]^{\bullet -} + Cl^- \quad (11')$$

The formation of μ-halide dimeric forms of the monomer [Re(CO)$_3$Br], having two bridging Br$^-$ ligands, has been shown in apolar solvents.[17] Such species are unstable in coordinating solvents, in which a fast bridge-splitting reaction takes place.[17] However, further stabilization in the case of {(bpy)Re···Cl···Re(bpy)}$^{3-}$ might derive from the lower oxidation state of the metal centers (Re^0). In light of the present hypothesis, the observed effect of Na$^+$ ions on the CV of [Re(CO)$_3$bpyCl] is ascribed to the unavailability of free Cl$^-$ ions to give the bridged intermediates in the reaction sequences 10 and 11/11′.

Surprisingly enough, addition of Cl$^-$ (TEACl) to DMF solutions of both [bpy(CO)$_3$Re−Re(CO)$_3$bpy] and [Re(CO)$_3$bpyACN]$^+$ under the conditions of Figures 7 and 8 did not significantly modify the CV pattern. A change of the shape of peak C should in fact have been expected. Although small modifications in the curve might be hidden by the overlapping of peak C with the oxidation peaks of the pristine species, as described above, the negative result would suggest that the solvent cage hinders the efficient interaction of the fragment [Re(CO)$_3$bpy]$^-$ with Cl$^-$ ions except when they are released from the complex *inside the solvent cage*.

Summarizing, the oxidation of [Re(CO)$_3$bpy]$^-$ may occur along two different pathways: (i) the homogeneous path represented by reactions 3 and 4; (ii) the heterogeneous path via the formation of intermediate **5** ({(bpy)Re···Cl···Re(bpy)}$^{3-}$). Path (i) would prevail under conditions in which the formation of **5** is hindered, that is, (a) low complex concentration, (b) absence of Cl$^-$ ions.

Attempts to isolate and further characterize species **5** (Scheme 1) were made by performing bulk electrolysis of a 1 mM solution of [Re(CO)$_3$bpyCl], 0.05 M TEATFB, DMF solution, at 25 °C at either −1.45 V (first reduction) or −1.80 V (second reduction) and recording the UV−vis−NIR spectra of the electrolyzed solutions. The electrolyses consumed 1 electron/molecule and 2 electrons/molecule, respectively. In the first case, an absorption band centered at 570 nm increased at the expense of the MLCT absorption band at 370 nm, with an isosbestic point at 400 nm. Upon reoxidation the absorption spectrum of pristine [Re(CO)$_3$bpyCl] was obtained. By contrast, the same experiment performed in ACN led to the formation of the dimer [bpy(CO)$_3$Re−Re(CO)$_3$bpy], as proved by the characteristic absorption bands at 454, 592, and 778 nm.[6c] This is in line with previous studies carried out in that solvent.[6] When the bulk electrolysis was performed, in DMF, in correspondence with the second reduction, no isosbestic point was observed, indicating the presence of more than two species in solution. The final spectrum did not show the characteristic absorption of either neutral or monoreduced dimer. Upon reoxidation (2 electrons/molecule) the original absorption spectrum was repristinated, thus showing that, in the long time scale of bulk electrolysis, species **7** (Scheme 1) is labile.

SCHEME 2

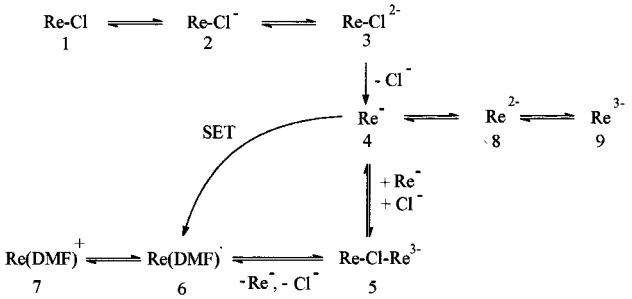

The failure to observe dimer formation in DMF was ascribed to the better ligating properties of DMF molecules with respect to ACN: the coordination of a solvent molecule by $[Re(CO)_3(bpy)]^{\bullet}$ would compete, in DMF, with its dimerization. In ACN, by contrast, dimerization would represent the fastest pathway for stabilizing the radical. According to this hypothesis, in DMF the redox processes associated with peaks VI/A and V/C would involve the solvato complex. The hypothesis is consistent with the reported behavior of $[Re(CO)_3bpyX]$ complexes (X = various monodentate ligands) as homogeneous catalysts in the electro- and photoinduced reduction of CO_2.[5g,h,6e] In these studies, usually carried out in ACN, it was shown that the main reason for the catalytic efficiency decrease is the dimerization of $[Re(CO)_3bpy]^-$, successive to the irreversible two-electron reduction of the catalyst. It was however shown that no loss of efficiency is observed when an excess of free coordinating anions such as Cl^- or ClO_4- is used. In this case, in fact, dimerization would not occur: the ligating anions would play, in ACN, the role played by solvent itself in DMF.

Finally, Scheme 2 summarizes the above discussion, assigning the proposed chemical identity to the species indicated in Scheme 1.

Correlation between Spectroscopic and Electrochemical Properties. This kind of correlation has found an extensive use for Ru(II), Os(II), and Re(I) complexes containing diimine ligands.[18,5l] It is a useful tool for obtaining absorption and emission energies from electrochemical data and vice versa. The basis for this correlation is that the orbitals involved in the optical transition are the same redox orbitals involved in the electrochemical processes. In the case of the MLCT transitions in the above complexes, a correlation is usually found with the potential difference between the first metal centered oxidation and the first diimine-ligand-centered reduction, $\Delta E_{1/2} = (E_{1/2ox} - E_{1/2red})$. In a previous study,[5l] relative to a large series of polypyridine$-Re^I(CO)_3Cl$ complexes, such a correlation was evidenced, but due to the irreversibility of the oxidation processes, only the ligand-centered reduction potentials were taken into account, assuming that $E_{1/2}$ was nearly the same along the series where the π_M orbital is relatively insensitive to the nature of the diimine ligand. In the case of the complexes studied in the present work, however, such an assumption cannot be made. As a matter of fact, a great shift in the $E_{1/2ox}$ is observed in the series of complexes, Table 1, and therefore $\Delta E_{1/2}$ has to be considered in the correlation.

The dimeric species $[bpy(CO)_3Re-Re(CO)_3bpy]$ and $[phen(CO)_3Re-Re(CO)_3phen]$ where also considered in the correlation. It has in fact been proved that the lowest transition for these species is an MLCT transition involving the σ_{Re-Re} and the diimine-ligand-centered π^* orbitals.[7d] The linear least-squares fit relative to the plot of $E_{mlct} = h\nu_{max,abs}$ (in eV) vs $\Delta E_{1/2}$ yields $E_{mlct} = 1.40\Delta E_{1/2} - 0.45$, $r = 0.99$. This result is in line with the expected behavior if, in first approximation, the redox orbitals are the same as those involved in the optical transition. Although a slope equal to unity should be expected, a value other than unity has already been observed in several cases.[18b] Several effects have been invoked for its explanation including solvation energies and hole$-$electron interaction energies in the excited state, which might vary along the series of complexes.[18b,d]

TABLE 1: $E_{1/2}$ Values (vs SCE) Relative to the First Oxidation and to the First Reduction for the Reported Species

	$E_{1/2}^{Iox}$/V	$E_{1/2}^{Ired}$/V
$[Re(CO)_3bpyCl]$	1.40	−1.38
$[Re(CO)_3phenCl]$[24]	1.41	−1.36
$[Re(CO)_3bpyCN]$	1.56	−1.30
$[Re(CO)_3phenCN]$	1.60	−1.42
$[Re(CO)_3bpyACN]^+$	1.79	−1.26
$[Re(CO)_3phenACN]^+$	1.82	−1.24
$[Re(CO)_3bpy]_2$[a]	−0.03	−1.56
$[Re(CO)_3phen]_2$[24]	0.01	−1.52

[a] The reversible one-electron oxidation of the dimer was observed at $\upsilon \geq 5$ V/s at −54 °C in DMF.

Conclusions

This work addresses the electrochemical and spectroscopic behavior of a family of mononuclear Re(I) complexes, $[Re^I(CO)_3LX]^{n+}$, with L = bpy, phen and X = Cl, CN ($n = 0$), ACN ($n = 1$), and of the metal$-$metal-bonded dimeric complexes $[(L)(CO)_3Re-Re(CO)_3(L)]$ (L = bpy, phen). The electrochemical study, carried out in strictly aprotic conditions, has allowed the observation of the largest number of redox processes so far obtained for these species and gives a detailed description of the kinetics of the electrode processes.

The reversible metal-centered oxidation of $[Re^I(CO)_3LX]$, with L = bpy, phen and X = Cl, CN, is only obtained at high scan rates, while at low scan rates the oxidation is irreversible and a two-peak pattern is observed. The first irreversible peak corresponds to a chloride- or cyanide-centered oxidation and the second one to the metal-centered oxidation in the resulting solvato complex. This was confirmed by comparison with the pristine $[Re^I(CO)_3L(ACN)]^+$. Solvent effects were not evidenced in the oxidative CV behavior of the above species, showing that the process is kinetically controlled by loss of Cl or CN radicals.

The cathodic behavior of the title species is characterized by four successive reduction peaks, of which the first, third, and fourth ones are reversible and the second chemically irreversible. The second reduction brings about the rapid cleavage of the metal$-$(pseudo)halogen or metal$-$metal bond, generating the same species in all cases, namely, $[Re(CO)_3bpy]^-$. Reoxidation of this fragment occurs either heterogeneously or homogeneously (involving the pristine species in different oxidation states), and competition between the two pathways is strongly influenced by the presence (or absence) of chloride ions.

A satisfactory description both qualitative and quantitative of the mechanism of oxidation and reduction processes was obtained by using CV, chronoamperometry, and controlled potential bulk electrolysis and by the extensive use of digital simulation of the CV curves, which confirmed the observed effects on the CV behavior due to changes in scan rate, temperature, concentration, and solvent.

Finally, the good linear correlation between spectroscopic and electrochemical data obtained considering both the monomeric and the dimeric complexes is in line with the expected behavior

if, in first approximation, the redox orbitals are the same as those involved in the optical transition.

Experimental Section

Preparations. *Materials.* Literature procedures were used to prepare the following complexes (L = bpy, phen): *fac*-[Re(CO)$_3$LCl],[4a,19a] *fac*-[Re(CO)$_3$L(ACN)],[4f,19a,b] *fac*-[Re(CO)$_3$LCN],[4n] and [L(CO)$_3$Re−Re(CO)$_3$L].[5d,6b,c,7d,19c]

ACN and CH_2Cl_2 (Aldrich) were dried by distillation over P_2O_5 under argon. THF was distilled from sodium benzophenone ketyl under argon. All other reagents were of reagent grade quality and were used without further purification. Rhenium precursors were obtained from Aldrich. Elemental analyses were performed by Ciba Laboratories (Bologna, Italy).

Electrochemical Experimental Procedures. *Materials.* All materials were reagent grade chemicals. Tetraethylammonium tetrafluoroborate (TEATFB), tetrabutylammonium hexafluorophosphate (TBAH), sodium tetrafluoroborate (NaTFB), or tetraethylammonium chloride (TEACl), all puriss. from Fluka, were used as supporting electrolytes as received. DMF (UVASOL, Merck), ACN (UVASOL, Merck), THF (LiChrosolv, Merck), CH_3NO_2 (Fluka), and CH_2Cl_2 (Fluka) were distilled into the electrochemical cell, prior to use, using a trap-to-trap procedure. The purification procedures relative to DMF and THF have previously been described.[3,20] The other solvents were transferred, under argon, from the original airtight containers into a Schlenk flask containing activated 4 Å molecular sieves and kept under vacuum prior to use.

Procedures. The one-compartment electrochemical cell was of airtight design with high-vacuum glass stopcocks fitted with either Teflon or Kalrez (DuPont) O-rings in order to prevent contamination by grease. The connections to the high-vacuum line and to the Schlenck containing the solvent were obtained by spherical joints also fitted with Kalrez O-rings. The pressure measured in the electrochemical cell prior to performing the trap-to-trap distillation of the solvent was typically $(2.0-3.0) \times 10^{-5}$ mbar. The working electrode consisted of a 0.6 mm-diameter platinum wire (0.15 cm^2 approximately) sealed in glass. The counter electrode consisted of a platinum spiral, and the quasi-reference electrode was a silver spiral. The quasi-reference electrode drift was negligible for the time required by a single experiment. Both the counter and the reference electrode were separated from the working electrode by ~0.5 cm. Potentials were measured with the ferrocene standard and are always referred to SCE.[20] $E_{1/2}$ values correspond to $(E_{pc} + E_{pa})/2$ from CV curves. The temperature-dependent ferrocinium/ferrocene couple standard potential was measured with respect to SCE by a nonisothermal arrangement according to the method outlined in ref 21. In some experiments a SCE reference electrode was used, separated from the working electrode compartment by a sintered glass frit. Ferrocene was also used as internal standard for checking the electrochemical reversibility of a redox couple.

Potential-controlled bulk electrolysis was carried out in a three-compartment electrochemical cell with both the SCE reference electrode and the platinum spiral counter electrode separated from the working electrode compartment by sintered glass frits. The working electrode was a large area platinum gauze. The electrolized solution was monitored at intervals during the electrolysis by voltammetry with periodical renewal of the diffusion layer,[22] and at the same time, UV−vis spectra were taken.

Digital Simulation of Cyclic Voltammetric Experiments. The CV simulations were carried out by using an explicit finite difference scheme making use of a commercially available software[23] opportunely modified for the simulation of repetitive cycles. All the electrochemical steps were considered fast in the simulation, and the simulation parameters were chosen so as to obtain a visual best fit over a 10-fold range of scan rates. This procedure allowed the assignment of the rate constants of the chemical steps with a 20% error.

Acknowledgment. This work was supported by the Ministero dell'Università e della Ricerca Scientifica e Tecnologica, by the Consiglio Nazionale delle Ricerche, by the University of Bologna (Funds for Selected Research Topics), by Ecole Normale Supérieure, the French Ministry of Research, and CNRS (URA 1679). F.P. would like to thank NATO (Grant No. 9413/84, Supramolecular Chemistry Special Programme) for a stay at the Ecole Normale Supérieure, Paris.

References and Notes

(1) (a) Strouse, G. F.; Schoonover, J. R.; Duesing, R.; Meyer, T. J. *Inorg. Chem.* **1995**, *34*, 2725. (b) Wang, Y.; Schanze, K. S. *Inorg. Chem.* **1994**, *33*, 1354. (c) Schanze, K. S.; MacQueen, D. B.; Perkins, T. A.; Cabana, L. A. *Coord. Chem. Rev.* **1993**, *122*, 63. (d) Connick, W. B.; Di Bilio, A. J.; Hill, M. G.; Winkler, J. R.; Gray, H. B. *Inorg. Chim. Acta* **1995**, *240*, 169. (e) Claude, J. P.; Williams, D. S.; Meyer, T. J. *J. Am. Chem. Soc.* **1996**, *118*, 9782. (f) Berg-Brennan, C. A.; Yoon, D. I.; Slone, R. V.; Kazala, A. P.; Hupp, J. T. *Inorg. Chem.* **1996**, *35*, 2032. (g) Lynam, M. M.; Vites, J. C. *Coord. Chem. Rev.* **1997**, *162*, 319.

(2) (a) Bignozzi, C. A.; Argazzi, R.; Chiorboli, C.; Roffia, S.; Scandola, F. *Coord. Chem. Rev.* **1991**, *111*, 261. (b) Argazzi, R.; Bignozzi, C. A.; Bortolini, O.; Traldi, P. *Inorg. Chem.* **1993** *32* 1222. (c) Argazzi, R.; Bignozzi, C. A.; Heimer, T. A.; Meyer, G. J. *Inorg. Chem.* **1997**, *36*, 2 and references therein.

(3) (a) Roffia, S.; Casadei, R.; Paolucci, F.; Paradisi, C.; Bignozzi, C. A.; Scandola, F. *J. Electroanal. Chem.* **1991**, *302*, 157. (b) Teixeira, M. G.; Roffia, S.; Bignozzi, C. A.; Paradisi, C.; Paolucci, F. *J. Electroanal. Chem.* **1993**, *345*, 243.

(4) (a) Wrighton, M.; Morse, D. L. *J. Am. Chem. Soc.* **1974**, *96*, 998. (b) Wrighton, M. S.; Morse, D. L., Pdungsap, L. *J. Am. Chem. Soc.* **1975**, *97*, 2073. (c) Morse, D. L.; Wrighton, M. S. *J. Am. Chem. Soc.* **1976**, *98*, 3931. (d) Luong, J. C.; Nadjo, L.; Wrighton, M. S. *J. Am. Chem. Soc.* **1978**, *100*, 5790. (e) Luong, J. C.; Faltynek, R. A.; Wrighton, M. S. *J. Am. Chem. Soc.* **1979**, *101*, 1597. (f) Luong, J. C.; Faltynek, R. A.; Wrighton, M. S. *J. Am. Chem. Soc.* **1980**, *102*, 7892. (g) Summers, D. P.; Luong, J. C.; Wrighton, M. S. *J. Am. Chem. Soc.* **1981**, *103*, 5238. (h) Westmoreland, T. D.; Le Bozec, H.; Murray, R. W.; Meyer, T. J. *J. Am. Chem. Soc.* **1983**, *105*, 5952. (i) Caspar, J. V.; Sullivan, B. P.; Meyer, T. J. *Inorg. Chem.* **1984**, *23*, 2104. (j) Meyer, T. J.; Caspar, J. V. *Chem. Rev.* **1985**, *85*, 187. (k) Kaim, W.; Kohlmann, S. *Chem. Phys. Lett.* **1987**, *139*, 365. (l) Juris, A.; Campagna, S.; Bidd, I.; Lehn, J.-M.; Ziessel, R. *Inorg. Chem.* **1988**, *27*, 4007. O'Toole, T. R.; Sullivan, B. P.; Meyer, T. J. *J. Am. Chem. Soc.* **1989**, *111*, 5699. (m) Kaim, W.; Kramer, H. E. A.; Vogler, C.; Rieker, J. *J. Organomet. Chem.* **1989**, *367*, 107. Sacksteder, L.; Zipp, A. P.; Brown, E. A.; Streich, J.; Demas, J. N.; DeGraff, B. A. *Inorg. Chem.* **1990**, *29*, 4335. (n) Leasure, R. M.; Sacksteder, L.; Nesselrodt, D.; Reitz, G. A.; Demas, J. N.; DeGraff, B. A. *Inorg. Chem.* **1991**, *30*, 3722. (o) Shaw, J. R.; Schmehl, R. H. *J. Am. Chem. Soc.* **1991**, *113*, 389. (p) Feliz, M.; Ferraudi, G. J.; Altmiller, H. *J. Phys. Chem.* **1992**, *96*, 257. (q) Feliz, M.; Ferraudi, G. *J. Phys. Chem.* **1992**, *96*, 3059. (r) George, M. W.; Johnson, F. P. A.; Westwell, J. R.; Hodges, P. M.; Turner, J. J. *J. Chem. Soc., Dalton Trans.* **1993**, 2977. (s) Abel, E. W.; Dimitrov, V. S.; Long, N. J.; Orrell, K. G.; Osborne, A. G.; Pain, H. M.; Šik, V.; Hursthouse, M. B.; Mazid, M. A. *J. Chem. Soc., Dalton Trans.* **1993**, 597. (t) Wallace, L.; Rillema, D. P.; *Inorg. Chem.* **1993**, *32*, 3836. (u) Moya, S. A.; Guerrero, J.; Pastene, R.; Schmidt, R.; Sariego, R.; Sartori, R.; Sanz-Aparicio, J.; Fonseca, I.; Martínez-Ripoll, M. *Inorg. Chem.* **1994**, *33*, 2341. (v) Rossenaar, B. D.; van der Graaf, T.; van Eldik, R.; Langford, C. H.; Stufkens, D. J.; Vlcek, A., Jr. *Inorg. Chem.* **1994**, *33*, 2865. (w) Lee, Y. F.; Kirchoff, J. R. *J. Am. Chem. Soc.* **1994**, *116*, 3599. (x) Oriskovich, T. A.; White, P. S.; Thorp, H. H. *Inorg. Chem.* **1995**, *34*, 1629. (y) Helberg, L. E.; Barrera, J.; Sabat, M.; Harman, W. D. *Inorg. Chem.* **1995**, *34*, 2033.

(5) (a) Haweker, J.; Lehn, J.-M.; Ziessel, R. *J. Chem. Soc., Chem. Commun.* **1983**, 536. (b) Sullivan, B. P.; Meyer, T. J. *J. Chem. Soc., Chem. Commun.* **1984**, 1244. (c) Kutal, C.; Weber, M. A.; Ferraudi, G.; Geiger, D. *Organometallics* **1985**, *4*, 2161. (d) Kalyanasundaram, K. *J. Chem. Soc., Faraday Trans. 2* **1986**, *82*, 2401. (e) Sullivan, B. P.; Meyer, T. J. *Organometallics* **1986**, *5*, 1500. (f) Hukkanen, H.; Pakkanen, T. T. *Inorg. Chim. Acta* **1986**, *114*, L43. (g) Haweker, J.; Lehn, J.-M.; Ziessel, R. *Helv. Chim. Acta* **1986**, *69*, 1990. (h) Ishitani, O.; Namura, I.; Yanagida, S.; Pac,

C. *J. Chem. Soc., Chem. Commun*. **1987**, 1153. (i) Kutal, C.; Corbin, A. J.; Ferraudi, G. *Organometallics* **1987**, *6*, 553. (j) Meyer, T. J. *Acc. Chem. Res*. **1989**, *22*, 163. (k) Collin, J. P.; Sauvage, J. P. *Coord. Chem. Rev*. **1989**, *93*, 245. (l) Pac, C.; Kaseda, S.; Ishii, K.; Yanagida, S. *J. Chem. Soc., Chem. Commun*. **1991**, 787. (m) Calzaferri, G.; Hädener, K.; Li, J. *J. Photochem. Photobiol. A: Chem.* **1992**, *64*, 259. (n) Ishitani, O.; George, M. W.; Ibusuki, T.; Johnson, F. P. A.; Koike, K.; Nozaki, K.; Pac, C.; Turner, J. J.; Westwell, J. R. *Inorg. Chem*. **1994**, *33*, 4712.

(6) (a) Haweker, J.; Lehn, J.-M-; Ziessel, R. *J. Chem. Soc., Chem. Commun*. **1984**, 328. (b) Sullivan, B. P.; Bolinger, C. M.; Conrad, D.; Vining, W. J., Meyer, T. J. *J. Chem. Soc., Chem. Commun*. **1985**, 1414. (c) Breikks, A. I.; Abruña, H. D. *J. Electroanal. Chem*. **1986**, *201*, 347. (d) Christensen, P.; Hamnett, A.; Muir, A. V. G.; Timney, J. A. *J. Chem. Soc., Dalton Trans*. **1992**, 1455. (e) Bakir, M.; McKenzie, J. A. M. *J. Electroanal. Chem*. **1997**, *425*, 61. (f) Yam, V. W.-W.; Wong, K. M.-C.; Cheung, K.-K. *Organometallics*, **1997**, *16*, 1729. (g) Hori, H.; Koike, K.; Ishizuka, M.; Takeuchi, K.; Ibusuki, T. *J. Organomet. Chem*. **1997**, *530*, 169.

(7) (a) O'Toole, T. R.; Margerum, L. D.; Westmoreland, T. D.; Vining, W. J.; Murray, R. W.; Meyer, T. J. *J. Chem. Soc., Chem. Commun*. **1985**, 1416. (b) Cosnier, S.; Deronzier, A.; Moutet, J.-C. *J. Electroanal. Chem*. **1986**, *207*, 315. (c) Cosnier, S.; Deronzier, A.; Moutet, J.-C. *J. Mol. Catal*. **1988**, *45*, 381. (d) O'Toole, T. R.; Sullivan, B. P.; Meyer, T. J. *J. Am. Chem. Soc.* **1989**, *111*, 5699. (e) O'Toole, T. R.; Sullivan, B. P.; Bruce, M. R.-M.; Margerum, L. D.; Murray, R. W.; Meyer, T. J. *J. Electroanal. Chem.* **1989**, *259*, 217. (f) Cosnier, S.; Deronzier, A.; Moutet, J.-C *New J. Chem.* **1990**, *14*, 831. (g) Snyder, S. R.; White, H. S.; López, S.; Abruña, H. D. *J. Am. Chem. Soc*. **1990**, *112*, 1333. (h) Yoshida, T.; Tsutsumida, K.; Teratani, S.; Yasufuku, K.; Kaneko, M. *J. Chem. Soc., Chem. Commun.* **1993**, 631. (i) Christensen, P.; Hamnett, A.; Muir, A. V. G.; Timney, J. A.; Higgins, S. *J. Chem. Soc., Faraday Trans.* **1994**, *90*, 459. (j) Ramos Sende, J. A.; Arana, C. R.; Hernández, L.; Potts, K. T.; Keshevarz-K, M.; Abruña, H. D. *Inorg. Chem*. **1995**, *34*, 3339.

(8) (a) Vlcek, A. A. *Coord. Chem. Rev*. **1982**, *43*, 39; (b) *Rev. Chim. Miner*. **1983**, *20*, 612.

(9) Juris, A.; Balzani, V.; Barigelletti, F.; Campagna, S.; Belser, P.; Zelewsky, A. *Coord. Chem. Rev*. **1988,** *85*, 85.

(10) Kuchynka, D. J.; Kochi, J. K. *Inorg. Chem*. **1988**, *27*, 2574 and ref 42 therein.

(11) Bard, A. J.; Faulkner, L. R. *Electrochemical Methods*; Wiley: New York, 1980; p 181.

(12) (a) Nicholson, R. S.; Shain, I. *Anal. Chem.* **1964**, *36*, 706. (b) Ref 11, p 443.

(13) Lee, K. Y.; Amatore, C.; Kochi, J. K. *J. Phys. Chem.* **1991**, *95*, 1285. Savéant, J.-M.; Vianello, E. *Electrochim. Acta* **1963**, *8*, 905.

(14) (a) Evans, D. H. *Chem Rev*. **1990**, *90*, 739. (b) Richards, T. C.; Geiger, W. E. *J. Am. Chem. Soc*. **1994**, *116*, 2028. (c) Guedes da Silva, M. F. C.; Fraústo da Silva, J. J. R.; Pombeiro, A. J. L.; Amatore, C.; Verpeaux, J.-N. *Organometallics* **1994**, *13*, 3943 and references 18−20 therein.

(15) Riddick, J.; Bruger, W. B.; Sakano, T. K. *Organic Solvents. Physical Properties and Methods of Purification*, 4th ed.; Wiley: New York, 1986.

(16) (a) Lee, K.-W.; Brown, T. L. *J. Am. Chem. Soc.* **1987**, *109*, 3269. (b) Astruc, D. *Electron Transfer and Radical Processes in Transition Metal Complexes*; VCH: New York, 1995.

(17) Vitali, D.; Calderazzo, F. *Gazz. Chim. Ital*. **1972**, *102*, 587.

(18) (a) Loutfy, R. O.; Loutfy, R. O. *Can. J. Chem*. **1976**, *54*, 1454. (b) Howell, J. O.; Goncalves, J. M.; Amatore, C.; Klasinc, L.; Wightman, R. M.; Kochi, J. K. *J. Am. Chem. Soc.* **1984**, *106*, 3968. (c) Juris, A.; Belser, P.; Barigelletti, F.; von Zelewsky, A.; Balzani, V. *Inorg. Chem*. **1986**, *25*, 256. (d) Barigelletti, F.; Juris, A.; Belser, P.; von Zelewsky, A. *Inorg. Chem*. **1987**, *26*, 4115.

(19) (a) Caspar, J. V.; Meyer, T. J. *J. Phys. Chem.* **1983**, *87*, 952. (b) Fredericks, S. M.; Luong, J. C.; Wrighton, M. S. *J. Am. Chem. Soc*. **1979**, *101*, 7415. (c) Kruck, T.; Hopfler, M.; Noach, M. *Chem. Ber*. **1966**, *99*, 1153.

(20) (a) Roffia, S.; Marcaccio, M.; Paradisi, C.; Paolucci, F.; Balzani, V.; Denti, G.; Serroni, S.; Campagna, S. *Inorg. Chem*. **1993**, *32*, 3003. (b) Paolucci, F.; Marcaccio, M.; Roffia, S.; Orlandi, G.; Zerbetto, F.; Prato, M.; Maggini, M.; Scorrano, G. *J. Am. Chem. Soc*. **1995**, *117*, 6572.

(21) Yee, E. L.; Cave, R. J.; Guyer, K. L.; Tyma, P. D.; Weaver, M. J. *J. Am. Chem. Soc.* **1979**, *101*, 1131.

(22) Farnia, G.; Roffia, S. *J. Electroanal. Chem*. **1981**, *122*, 347.

(23) Gosser, D. K. *Cyclic Voltammetry. Simulation and Analysis of Reaction Mechanisms*; VCH: New York, 1993.

(24) Roffia, S.; Marcaccio, M.; Paradisi, C.; Paolucci, F. Work in preparation.